Integrated Solenoid-Type Inductors for High Frequency Applications and Their Characteristics

Yong-Jun Kim[1] and Mark G. Allen[2]

[1]Samsung Electronics Co., Ltd., Core Technology Research Center, 416 Meatan-3Dong, Paldal-Gu,
Suwon City, Kyungki-Do, Korea
e-mail: yjk@secns.sec.samsung.co.kr

[2]School of Electrical and Computer Engineering, Georgia Institute of Technology,
791 Atlantic Drive NW, Atlanta, Georgia 30332-0269
e-mail: mallen@ee.gatech.edu

Abstract

New solenoid-type integrated inductors for high frequency applications have been realized using a surface micromachining technique and a polymer sacrificial layer, and their geometrical characteristic have been investigated. In general, integrated inductors can suffer from low Q factors and/or self-resonant frequencies when compared to their discrete counterparts. A spiral-type inductor, one of the dominant choices as an integrated inductor, requires relatively large two-dimensional spaces. In addition, the direction of flux of the spiral type inductor is perpendicular to the substrate, which can cause more interference with underlying circuitry or other integrated passives in a vertically stacked multi-chip modules (MCM). The proposed inductor in this research has an air core to reduce unwanted stray capacitance that can be added due to a magnetic core, and electroplated copper coil to reduce the series resistance. An important feature of the proposed inductor geometry is introducing an air gap between the substrate and the conductor coil in order to reduce the effects of the substrate dielectric constant. This air gap can be realized using a polyimide sacrificial layer and a surface micromachining technique. Therefore, the resulting inductor can have less substrate-dependent magnetic properties, less stray capacitance, and higher Q-factor. Inductors with different geometrical aspects, such as air gap height, core size, and number of turns, have been designed and fabricated on ceramic substrates. A variational study of these inductors has been performed to assess the impact of the geometrical aspects to the inductor performance at high frequency. The measured inductance of these inductors varies from 2nH to 20 nH, and maximum Q-factor 10-60.

Introduction

Realization of good quality integrated passives has been one of the key research areas in packaging and MMIC applications. Due to its three-dimensional nature, it was very hard to realize an integrated inductor with conventional two-dimensional microfabrication techniques. Recently, there has been much research to realize various integrated inductors[1-4]. Most of the conventional geometries for integrated inductors have been meander-types or spiral-types[1,5], whereas most of the macro-scale inductors are solenoid-types. The main reason for not using a solenoid-type geometry for integrated inductors is the limitation of microfabrication techniques. Fabrication of a conductor coil wrapped around a core has been more difficult using conventional IC processes than the fabrication of meander or spiral-types. A meander-type inductor is simple to fabricate but, because of negative turn-to-turn mutual inductance, it suffers from low overall inductance. A spiral-type inductor, widely used as an integrated inductor, has relatively high inductance, but has several other drawbacks. First, it requires a lead wire to connect from the inside end of the coil to the outside, which introduces an unnecessary capacitance between the conductor and the lead wire, and this capacitance is one of the dominant stray capacitances of this geometry [5]. Second, its size is large compared with other inductor types with the same number of turns. Third, the direction of flux is perpendicular to the substrate, which can interfere with the underlying circuit in multi-chip modules or some vertically integrated devices.

The problems of spiral-type inductors can be solved with solenoid-type inductors. Previously, a fully integrated solenoid-type inductor, fabricated using various micromachining techniques and polymer/metal multilayer processing techniques, has been reported[6]. This inductor had an electroplated Ni-Fe permalloy core, and electroplated copper layers were used as conductors to reduce the coil resistance.

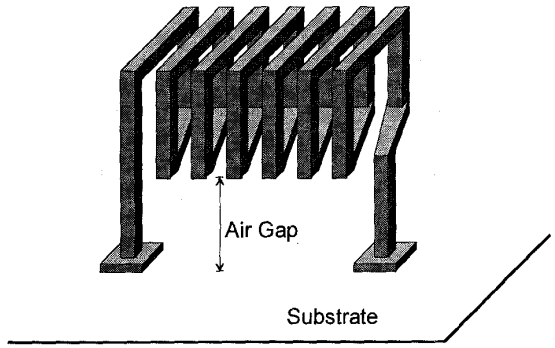

Figure 1. A schematic of an integrated solenoid-type inductor with an air gap.

In this work, an integrated inductor for high frequency applications based on solenoid geometries was designed and fabricated using polymer/metal multilayer processing and surface micromachining techniques. This inductor uses an air core and introduces an air gap between the substrate and the conductor. The air gap was realized using a surface micromachining technique with an organic sacrificial layer. This geometry will provide the inductor with more compact size, lower stray capacitance, and higher Q-factor. This inductor can be fabricated using low-temperature fabrication processes, allowing the possibility of fabrication on a wide variety of substrates, such as, silicon, GaAs, ceramic or organic (laminate) substrates, as a post processing .

Design Considerations

A conductor layer composed of low resistivity metal is critical to maintain a high inductor Q-factor at very high frequencies. This is due to the skin effect whereby high frequency currents flow only in the surface layer of the conductor. As a result, the DC resistance of the conductor will not provide an accurate indication of its resistance to the high frequency current. Since the metals of lower resistivity ρ are silver, copper, and gold, these are proper materials for the conductor coil. Electroplated copper was chosen for the conductor coil.

For a solenoid-type inductor, neglecting the effect of the substrate and fringing, the inductance L can be represented with a simple equation:

$$L = \frac{N^2 \mu A_c}{l_c}, \qquad (1)$$

where A_C is the cross-section area of the core, l_C is the total length of the core, μ is the permeability of the core, and N is the number of coil turns. In order to increase the inductance, L, in a given two-dimensional area, the area of the core, A_C, can be increased, which requires a tall via structure. Therefore, a high aspect-ratio, i.e., height-to-width ratio metal structure, as tall as current microfabrication techniques allow, must be used to achieve highest inductance and Q-factor for a given total inductor area.

In terms of fabrication complexity, the solenoid-type inductor is more complex than the spiral-type inductor. Since solenoid-type inductors require a gap between the bottom and top conductor (unlike spiral-types, which have only gaps between underlying conductors), additional stray capacitance components between the top and bottom conductors must be considered in the design stage. Large gaps between top and bottom conductors, i.e. tall vias, will increase the inductance and decrease the stray capacitance. Since most current microfabrication techniques are based on two-dimensional geometry, achieving a very high aspect ratio metallic structure is often difficult. In addition, very precise dimensional control is required to control the characteristics of these microinductors. Since this device includes no magnetic materials, its inductance value strictly depends on its geometry. Since high aspect ratio vias and tight geometry control are required simultaneously, the correct understanding of available microfabrication techniques and good expectation of geometric tolerance of available photolithographic methods and plating profile is critical in the design stage.

Stray capacitance determines the self resonant frequency (SRF), hence the inductor operation range and Q-factor of the inductor. Thus, controlling this capacitance is very important in the design stage and actual fabrication stage. Yamaguchi *et al.* [5] have reported calculated results for the stray capacitance of various parts of thin film inductors employing meander and spiral-type coils. It was reported that the capacitance between conductor lines was very small compared with that caused by the substrate-to-conductor. In an air-core inductor, where the only stray capacitances are conductor-to-conductor and conductor-to-substrate, reducing the conductor-to-substrate stray capacitance by introducing an air gap between the substrate and the coil can significantly lower the total stray capacitance. This air gap can be achieved with a surface micromachining technique using a polyimide sacrificial layer. Also, a coil geometry has been utilized which minimizes unnecessary stray capacitance between conductors by eliminating the overlaps between the top and the bottom conductor lines.

In order to estimate the stray capacitance characteristics of the inductor with various geometrical factors, a simple equivalent circuit model (Figure 2) is introduced. In this model only conductor-to-conductor capacitances were considered. Also this model is built on the assumption that the inductor coil is suspended in the air and the via conductors have no effect on the total stray capacitance. C_t is the capacitance between two top conductor lines, C_b between two bottom conductor lines, C_{bt} between the top and the bottom conductor lines, and C_x between two diagonally placed conductor lines (Figure 2). Neglecting fringing, these capacitances can be approximated as:

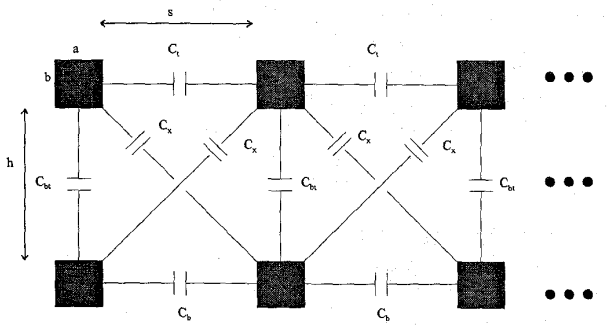

Figure 2. An equivalent circuit model for estimation of the stray capacitance between conductor lines. The cross-sectional area of the conductor lines and the capacitances between these conductor lines are shown.

$$C_t = C_b = \frac{\varepsilon A}{d} = \frac{\varepsilon(w \cdot b)}{s},$$
$$C_{bt} = \frac{\varepsilon(w \cdot a)}{h}, \qquad (2)$$
$$C_x = \frac{\varepsilon(w \cdot \sqrt{a^2 + b^2})}{\sqrt{s^2 + h^2}},$$

where ε is the dielectric constant of air, a is the width of a conductor line, b is the height of the conductor line, w is the length of each conductor lines, s is the horizontal spacing between each conductor lines, and h is the vertical spacing (via) between the top and the bottom conductor lines. After calculating each of the capacitances between conductor lines, these calculated values have been substituted in the circuit model in Figure 2. The total capacitance of the model is then calculated using a circuit simulation program, and this total capacitance can be interpreted as the stray capacitance of the inductor. The evaluation of C_t, C_{bt}, and C_x was used to pick a proper range of coil geometry.

Fabrication

The fabrication starts with an unpolished 2" by 2" alumina substrate coated with 30μm DuPont PI-2611 polyimide on one side (Figure 3). Multiple coating of DuPont PI-2611 on a seed layer produces a 20 μm thick PI layer. A support pattern to sustain the air gap between the substrate and the coil is defined using conventional photolithography techniques and wet etching techniques. The PI layer is etched with 100 % O_2 RIE, and, using this as a mold, electroplated Cu is deposited (a).

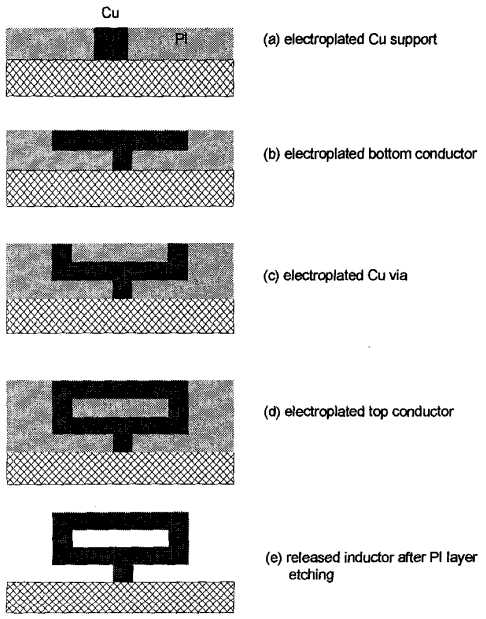

Figure 3. Simplified fabrication process.

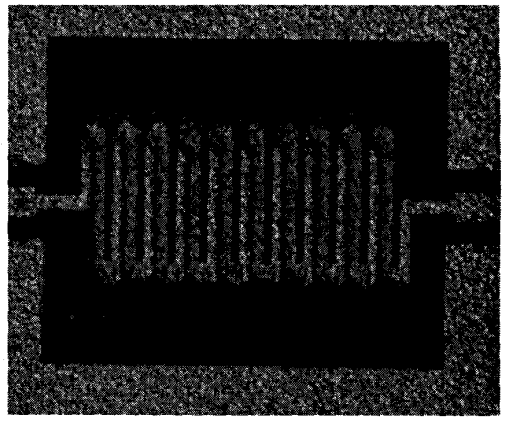

Figure 4. A top-view of an integrated solenoid-type inductor with a ten turn copper coil fabricated on an alumina substrate.

A new PI layer for bottom conductor pattern is formed and defined on a seed layer. Same electroplating technique is applied to form the bottom copper conductor layer(b). A 30μm thick via hole patterns are formed with 100% O_2 RIE and Cu vias are electroplated through these via holes(c). With the same method as above, top conductor pattern is formed with electroplated copper(d). The remaining polyimide layers are removed with an RIE etching technique, and all the seed layers are removed(e) with wet etching processes.

Figure 4 shows a top-view of an integrated inductor with a ten turn coil fabricated on an alumina substrate. Figure 5 shows a scanning electron microscoph (SEM) picture of a finished inductor suspended over the substrate. This picture clearly shows the air gap and the air core. High aspect ratio vias were used to increase the inductance and to decrease the stray capacitance between the top and the bottom conductor lines. Up to 1.5:1 aspect-ratio vias have been fabricated using a polymer/metal multilayer and high aspect-ratio via formation, as shown in Figure 6. Since the magnetic properties of the air-core inductors are determined by only its geometry, special care is needed in controlling the error margin in each photolithography and etching stage.

Measurements and Results

Various integrated inductors with different geometries, such as the number of turns and core sizes, were fabricated. Figure 7 is an equivalent circuit model of the inductor[7]. In this model, the combination of R_1, R_2, L_1, and L_2 represents the resistance change with frequency due to the skin effect, and the capacitor C is the effective total capacitance across the inductor.

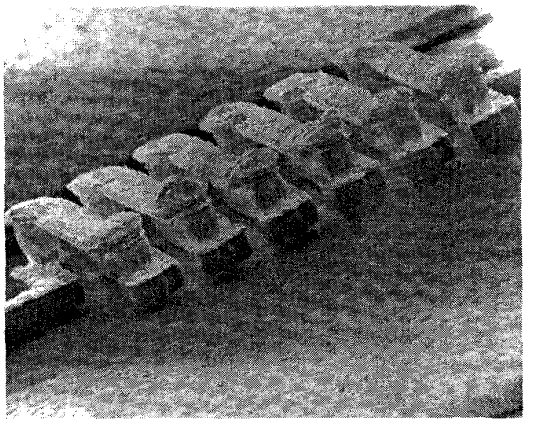

Figure 5. Scanning electron micrographs of the solenoid-type inductors suspended over the substrate by 20 μm.

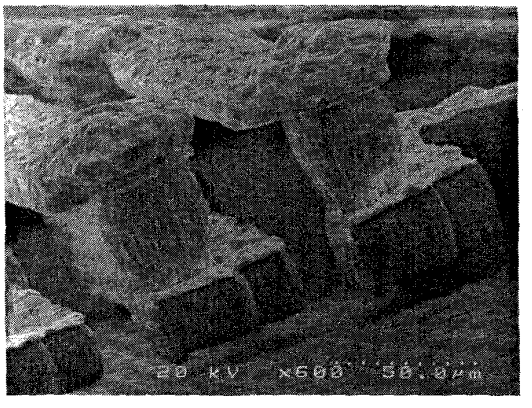

Figure 6. Scanning electron micrograph showing high aspect-ratio (1:1.5) vias.

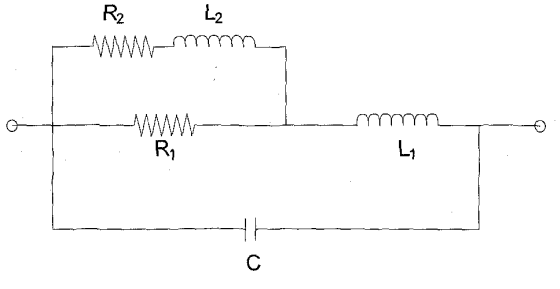

Figure 7. Equivalent circuit model of the inductor.

The samples have been measured using an HP 8510C Vector Network Analyzer and CASCADE MICROTECH ground-signal-ground high frequency coplanar probes with 100μm pitch size. The inductors were designed to have two-ports surrounded by a ground plane. The two-port S parameter measurements were averaged and then a π-network was generated according to the measured S-parameters. The unloaded input impedance was computed and the unloaded Q-factor was determined by dividing the imaginary part by the real part of the input impedance.

To remove the effect of the measurement parasitics, open-pads without inductors were designed and fabricated on the same substrate with the inductors. The measured S-parameters of the open-pad were interpreted as a series R and C circuit, and the R and C values were used to de-embed the open-pad from the inductor. The de-embedding and lumped parameter extraction has been performed by using an HP Microwave and RF Design System (MDS). The lumped parameter extraction has been accomplished with a non-linear optimization algorithm that employs a hybrid-optimization in MDS.

Geometrical parameters of a solenoid-type inductor have been illustrated in Figure 8. These inductors have 20μm wide (*a*) and 20μm thick (*b*) electroplated copper conductor lines, and the spacing (*s*) between each turns is 50μm. The vias have 33μm height (*h*), and the cross-section area of the vias is 30μm by 60μm. All inductors have 20μm air gaps (*g*). Since the conductor width (*a*) and the spacing (*s*) are constant, the total inductor length (core length) is proportional to the number of coil turns (*N*), and this can be represented as, $Core\ Length = 2(s+a)$. The core length varies with the number of turns and they are 400, 720, and 1520 μm for 6, 10, and 20 turn inductors, respectively. Typical dc resistance value varies from 0.32 to 1 Ω, inductance from 1 to 8 nH and stray capacitance from 13 to 30 fF. The smallest inductor has a self resonant frequency of 25 GHz.

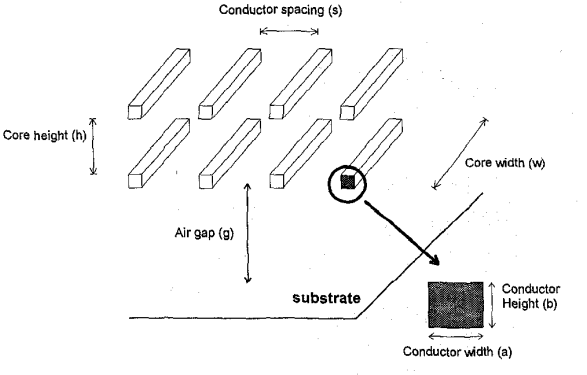

Figure 8. Geometrical parameters for solenoid-type inductors.

Figure 9 shows the effect of a 20 μm air gap, which shows the improvement of the electrical properties of the inductor. The stray capacitance has been reduced from 25.1 fF, with no air gap, to 17.7 fF, with a 20μm air gap. It is shown that the inductor with an air gap has higher Q-factors and SRF than the one without any air gap. Also, the inductor with an air gap has better inductance stability. Figure 10 represents the effect of the number of turns on the Q-factor and inductace. Obviously, increasing the turns increases the inductance, as can be expected from equation (1). But this increases the resistance and the stray capacitance of the inductor, which lowers the SRF and Q-factors. Figure 11 shows the effect of the core size by varying the core width (w). These inductors have the same number of turns (N), therefore all have the same core length. The increase in the core width (w) increases the inductance, because it increase the core cross-sectional area, as shown in equation (1). But the increase in w also increases the stray capacitance between the top and bottom conductor lines and the series resistance due to the increased overall coil length, resulting lower Q-factor and lower self resonant frequency.

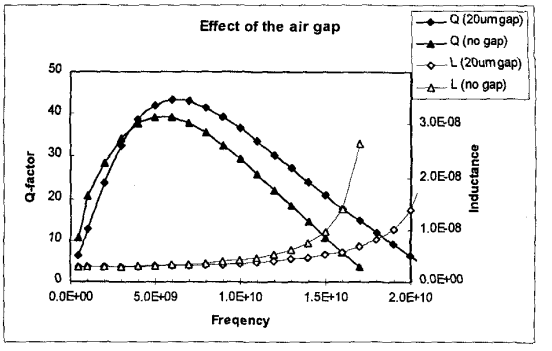

Figure 9. Effect of the air gap. The stray capacitance has been reduced from 25.1 fF, with no air gap, to 17.7 fF, with an 20μm air gap.

Conclusions

A surface micromachined integrated solenoid-type inductor for high frequency applications has been proposed and fabricated using polymer/metal multilayer processing techniques and surface micromachining techniques. To achieve high Q-factor, this inductor has solenoid-type geometry with an air core and introduces an air gap between the substrate and the conductor, which reduces stray capacitance contributed by the high dielectric constant of the substrate. This air gap was realized by using an organic sacrificial layer and releasing with a dry etching technique. The metal support maintaining the air gap can be an extension of the connection between underlying circuitry and the inductor.

Also, various factors of inductor geometries have been investigated by designing and fabricating several inductors with various geometry. A large air core generated with increased core width (w) can help to increase the inductance, but this also contributes to the stray capacitance increase. This stray capacitance increase reduces the resonant frequency and the Q-factor. Therefore highest aspect-ratio vias (h), as tall as current fabrication processes permit, is needed to achieve maximum inductance and Q-factor. In addition, the effect of the air gap to the inductor characteristics has been demonstrated.

Even though these solenoid-type inductors can have a drawback, increased fabrication complexity, these inductors have very good electrical properties such as high inductance and high Q-factors for a given 2-dimensional inductor area. Therefore, these inductors can find applications where inductors of compact size and good electrical properties are required.

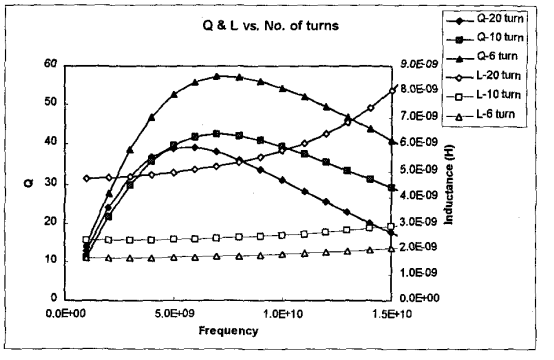

Figure 10. Q and inductance of inductors with different number of turns.

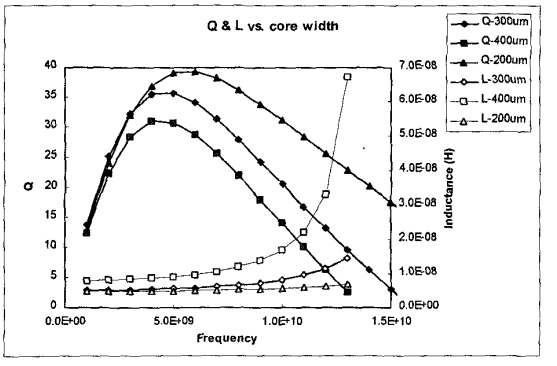

Figure 11. Q and inductance of inductors with different core sizes.

Acknowledgments

The authors would like to thank Dr. Joy Laskar and Dr. David R. Hertling of Georgia Tech. for valuable technical discussions, Mr. Seung-Yup Yoo and Mr. Sangwoo Han for the help in measurement, and Dr. K. Martin for the mask fabrication. Microfabrication was carried out at the Georgia Institute of Technology Microelectronics Research Center (MiRC). The authors wish to thank the MiRC staff for their assistance.

References

1. A. C. Reyes, S. M. El-Ghazaly, S. J. Dorn, M. Dydyk, D. K. Schroder, and H. Patterson, "Coplanar Waveguides and Microwave Inductors on Silicon Substrates", IEEE Trans. on Microwave theory and tech., Vol. 43, No.9, 2016-2022, Sep. 1995
2. D. Lovelace, N. Camilleri, and G. Kannell, "Silicon MMIC Inductor Modeling for High Volume, Low Cost Applications", Microwave Journal, 60-68, Aug. 1994
3. M. Hirano, Y. Imai, I. Toyoda, K. Nishikawa, M. Tokumitsu, and K, Asai, "Three-Dimensional Passive Elements for Compact GaAs MMICs", IEICE Trans. Electron., Vol. E76-c, No.6, 961-967, 1993
4. O. Oshiro, H. Tsujimoto, and K. Shirae, "High Frequency Characteristics of a Planar Inductor and a Magnetic Coupling Control Device", IEEE Translation J. Magnetics in Japan, Vol. 6, No. 5, 436-442, Mar. 1993
5. M. Yamaguchi, M. Matsumoto, H. Ohzeki and K. I. Arai, "Analysis of the inductance and the stray capacitance of the dry-etched micro inductors", IEEE Trans. Magnetics, Vol. 27, No 6, 5274-5276, Nov. 1991
6. C. H. Ahn, Y. J. Kim and M. G. Allen, "A fully integrated planar toroidal inductor with a micromachined nickel-iron magnetic bar", IEEE Trans. on Components, Packaging, and Manufacturing Technology, Part A, vol.17, no.3, p.463-9, Sep. 1994
7. Triquint Semiconductor "Gallium Arsenide IC Design Manual - GaAs QED/A process", version 3.0, OCT 1991
8. S. Hara, et al., "Broad-band monolithic microwave active inductor and its application to miniaturized wide-band amplifiers", IEEE Transactions on Microwave Theory and Techniques, vol.36, no.12, p.1920-4, Dec. 1988.